

(B) When $\nu > 0$, the stationary probability distribution becomes divergent at $x=0$. This result is clearly not realistic. Thus, a more realistic stochastic model should be proposed.

(C) In the region $x > 0$ the straight lines $\nu=0$ and $\nu=1$ give marginal situation, that is, the fluctuating intermediate undergoes the pitchfork bifurcation by crossing the lines and thus the variation of probability distributions becomes discontinuous, when the system undergoes the pitchfork phase transition.

(D) When a system has the same multiplicative noise and linear part of deterministic term, the same pitchfork bifurcations occur.^{1,2,7} The reason is that $\nu=0$ and $\nu=1$ lines are due to the noise and coupling between noise and linear part, respectively.

(E) The diffusion coefficient with ν induces the saddle-node bifurcation in the case of $x > 0$ and $0 < \nu < 1$. Below the curve of the saddle-node bifurcation the coupling between the drift and noise terms plays the most important role. However, the multiplicative noise term becomes dominant above the curve. Thus, it is clear that the variation of probability distributions is continuous.

(F) It should be very careful to apply the Ito or Stratonovich FPE to an actual system.²

(G) $\nu=1$ is the critical dynamic exponent. At $\nu \geq 1$ it is impossible that the intermediate for the Schlögl model with the second order transition near the stable steady state escapes over the unstable steady state of the potential barrier. For the model with the first order transition the transition rate from one stable steady state to the other stable state

through the unstable state become zero,¹ if $\nu \geq 1$. Also, the relaxation time for the models becomes infinite when $\nu=1$.

Some of the above results are unrealistic. Maybe the multiplicative noise should be expressed by a polynomial of the concentration of the intermediate instead of $|x|^\nu$. The reason is that starting from the master equation for the Schlögl model, the diffusion term in the FPE is expressed in terms of a polynomial of concentration.⁵ Investigation on this aspect is in progress in our group.

Acknowledgments. This work was supported by a grant (No. BSRI-93-311) from the Basic Science Research Program, Ministry of Education of Korea, 1993.

References

1. Kim, C. J.; Lee, D. J. *Bull. Korean Chem. Soc.* **1993**, *14*, 95.
2. Kim, K. R.; Lee, D. J.; Shin, K. J.; Kim, C. J. *Bull. Korean Chem. Soc.* **1994**, *15*, 631.
3. Schlögl, F. *Z. Phys.* **1971**, *248*, 446; **1972**, *252*, 147.
4. Kim, K. H.; Shin, K. J.; Lee, D. J.; Ko, S. B. *Bull. Korean Chem. Soc.* **1986**, *6*, 295.
5. Risken, H. *The Fokker-Planck Equations*; Springer-Verlag: New York, U. S. A., 1984.
6. We may improve the escape rate by expanding the higher order terms.⁵ However, the most important term is the exponential function and the improved parts describe only minor effect. Thus, we have neglected the improved parts.
7. Hu, G.; He, K. *Phys. Rev.* **1992**, *A45*, 5447.

Study of the Nonstoichiometry and Physical Properties of the $\text{Nd}_{1-x}\text{Sr}_x\text{FeO}_{3-y}$ System

Chul Hyun Yo*, Hyung Rak Kim, Kwang Hyun Ryu, Kwon Sun Roh, and Jin Ho Choy†

Department of Chemistry, Yonsei University, Seoul 120-749, Korea

†Department of Chemistry, Seoul National University, Seoul 151-742, Korea

Received March 22, 1994

The nonstoichiometric perovskite solid solutions of the $\text{Nd}_{1-x}\text{Sr}_x\text{FeO}_{3-y}$ system for the compositions of $x=0.00, 0.25, 0.50, 0.75,$ and 1.00 have been prepared at 1150°C in the air pressure. The compound of $x=0.00, \text{NdFeO}_{3.0}$, contains only Fe^{3+} ion in octahedral site and the others involves the mixed valence state between Fe^{3+} and Fe^{4+} ions. The mole ratio of Fe^{4+} ion or the τ -value increases steadily with the x -value and then is maximized at the composition of $x=1.00$. The nonstoichiometric chemical formulas of the system are formulated from the $x, \tau,$ and y values. From the Mössbauer spectroscopy, the isomer shift of Fe^{3+} ion decreases with the increasing x -value, which is induced by the electron transfer between the Fe^{3+} and Fe^{4+} ions. The transfer is made possible by the indirect interaction between Fe^{3+} and Fe^{4+} ions *via* the oxygen ion. The e_g electrons of the Fe^{3+} ions are delocalized over all the Fe ions. Due to the electron transfer, the activation energy of electrical conductivity is decrease with the increasing amount of Fe^{4+} ion.

Introduction

In the perovskite-type ABO_3 compound, the transition me-

tal placed in B-site is able to have higher valence state which is generally stabilized with a large A-site ion. The perovskite-type compounds have been studied extensively because of

their unique and applicable properties.¹⁻⁵ It has been found that a compound of orthoferrite type has an antiferromagnetic interaction of $\text{Fe}^{3+}\text{-O}^{2-}\text{-Fe}^{4+}$ which can be explained by the superexchange model. According to the previous studies of the orthoferrite type compounds, they exhibit weak ferromagnetism due to the distorted octahedra (FeO_6) along the c -axis.⁶⁻⁸ Takeda *et al.*⁹ have suggested that the SrFeO_3 has antiferromagnetism below the Néel temperature of 130 K. It has also been shown by using the neutron diffraction method that the Fe^{4+} ion within the octahedral site is stabilized with a low spin state ($t_{2g}^4e_g^0$) in $\text{SrFeO}_{2.9}$ using the neutron diffraction method.¹⁰ Gibb¹¹ has explained that the thermally activated electron transfer process in the SrFeO_{3-y} system takes place and results in a single narrow resonance line in Mössbauer spectroscopy.

The electrical conduction of perovskite materials has been affected by the interaction between the iron cation and the oxygen anion. The degree of the Fe-O-Fe interaction affects directly the carrier mobility.¹¹ When the Fe^{4+} ion is produced as a mixed valence state in a perovskite compound, the fast electron transfer between the Fe ions occurs by thermal excitation.^{2,3,11,13} In the perovskite compounds, ABO_3 , the higher oxidation state of B-site or the oxygen vacancies can be produced by the divalent cation substitution for the trivalent cation on the A-site. The oxygen vacancies as well as the B-site ion of the mixed valence states affect the B-O-B interaction considerably.³

In the $(\text{AA}')\text{FeO}_3$ system, the mixed valence state of the Fe ions might be formed depending on the valence states of A' ions and sample preparation conditions. The valence states of Fe ions will become a main factor of the physical properties for the perovskite compounds. In the present study, the nonstoichiometric chemical formulas of the $\text{Nd}_{1-x}\text{Sr}_x\text{Fe}^{3+}_{1-\tau}\text{Fe}^{4+}_\tau\text{O}_{3-y}$ system could be formulated through the chemical analysis. The bonding character of FeO and the mixed valence state of the Fe ions are investigated by using the Mössbauer spectroscopy. The magnetic and electrical properties are discussed with relation to the valence state of the Fe ions, the oxygen vacancies, and the degree of the interaction between the Fe ions.

Experimental

The solid solutions of the $\text{Nd}_{1-x}\text{Sr}_x\text{FeO}_{3-y}$ ($x=0.00, 0.25, 0.50, 0.75,$ and 1.00) system have been prepared from evaporating and firing the nitric acid solution of appropriate starting materials such as SrCO_3 , Nd_2O_3 , and ferric nitrate and then heating at 1200°C under the air pressure for 72 hrs. The products were ground, pressed into disks, and heated again in the same conditions for 24 hrs. The polycrystalline pellets were used for the electrical conductivity measurements.

By the XRD analysis with monochromatized $\text{Cu K}\alpha$ ($\lambda=1.5418 \text{ \AA}$) radiation, we confirmed whether the samples were formed into the solid solutions, and determined the lattice parameters and the crystal system. The mixed valence state between the Fe^{3+} and Fe^{4+} ions was determined and identified by Mohr salt analysis²⁶ and Mössbauer spectroscopy, respectively. The thermal analysis was carried out in the range of $300\text{--}1000 \text{ K}$. The Mössbauer spectra using the γ -ray source of ^{57}Co diffused within the Rh matrix were recorded in the room temperature. From the Mössbauer spec-

Table 1. Lattice Parameters and Crystal System of the $\text{Nd}_{1-x}\text{Sr}_x\text{FeO}_{3-y}$ Solid Solutions

x value	Lattice parameter ($\pm 0.001 \text{ \AA}$)			Crystal system
	a	b	c	
0.00	5.624	5.619	7.625	Orthorhombic
0.25	5.588	5.687	7.524	Orthorhombic
0.50	5.588	5.686	7.505	Orthorhombic
0.75	3.858	—	—	Cubic
1.00	3.855	—	—	Cubic

Table 2. x, τ, y Values, and Nonstoichiometric Chemical Formula of the $\text{Nd}_{1-x}\text{Sr}_x\text{Fe}^{3+}_{1-\tau}\text{Fe}^{4+}_\tau\text{O}_{3-y}$ System

x value	τ value (± 0.005)	y value	Nonstoichiometric chemical formula
0.00	0.00	0.00	$\text{NdFeO}_{3.00}$
0.25	0.22	0.01	$\text{Nd}_{0.75}\text{Sr}_{0.25}\text{Fe}^{3+}_{0.78}\text{Fe}^{4+}_{0.22}\text{O}_{2.99}$
0.50	0.38	0.06	$\text{Nd}_{0.50}\text{Sr}_{0.50}\text{Fe}^{3+}_{0.62}\text{Fe}^{4+}_{0.38}\text{O}_{2.94}$
0.75	0.44	0.15	$\text{Nd}_{0.25}\text{Sr}_{0.75}\text{Fe}^{3+}_{0.56}\text{Fe}^{4+}_{0.44}\text{O}_{2.85}$
1.00	0.47	0.27	$\text{SrFe}^{3+}_{0.53}\text{Fe}^{4+}_{0.47}\text{O}_{2.73}$

troscopic analysis, we are able to discuss about the interaction between the Fe ions and about the electric field gradient produced by the oxygen vacancies. The magnetic measurements were also carried out $4\text{--}800 \text{ K}$ in the air. The electrical conductivities of the samples had been measured by the four probe DC technique in the temperature range of $78\text{--}900 \text{ K}$ under the air pressure. The electrical conductivities were calculated by the Laplume's equation.

Result and Discussion

The x-ray diffraction patterns of the compounds, $x=0.00, 0.25,$ and 0.50 are indexed on the basis as the an orthorhombic system as the orthoferrite which is distorted perovskite type structure. The compositions of $x=0.75$ and $1.00,$ however, are assigned to the cubic structure. A distortion of the axis of the octahedra is reduced by replacing the Nd^{3+} ion with Sr^{2+} ion which has larger ionic radius than Nd^{3+} ion. The lattice parameters and crystal system of each composition are listed in Table 1.

The mole ratio of Fe^{4+} ions to the total Fe ions or the τ -value is measured by Mohr salt analysis and then the amount of oxygen vacancies or the y ($y=(x-\tau)/2$) is calculated. Therefore, the nonstoichiometric chemical formulas of the $\text{Nd}_{1-x}\text{Sr}_x\text{Fe}^{3+}_{1-\tau}\text{Fe}^{4+}_\tau\text{O}_{3-y}$ system corresponding to each composition are formulated as listed in Table 2. The compound of $x=0.00,$ $\text{NdFeO}_{3.00},$ has only Fe^{3+} ion and the others have the mixed valence state between the Fe^{3+} and Fe^{4+} ions. The τ and y values increase with the x -value for the system as shown in Figure 1.

The experimental data of DTA show that the compound of $x=0.00$ has small endothermic peak about 300 K and the others have no such peaks. In the case of $x=1.00,$ the endothermic peak may show a structural transition from the bro-

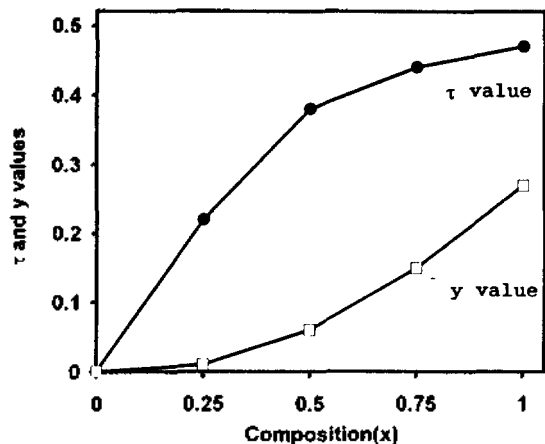


Figure 1. Plot of the τ and y values vs. x value for the $\text{Nd}_{1-x}\text{Sr}_x\text{Fe}^{3+}_{1-y}\text{Fe}^{4+}_y\text{O}_{3-y}$ system.

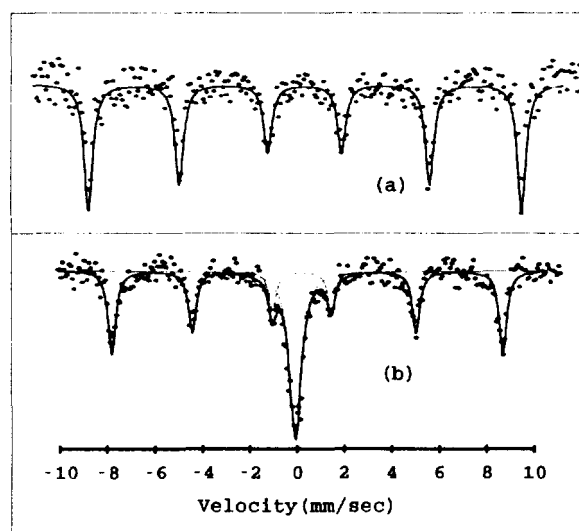


Figure 2. Mössbauer spectra for the $\text{Nd}_{1-x}\text{Sr}_x\text{FeO}_{3-y}$ system at the room temperature: (a) $\text{NdFeO}_{3.0}$ and (b) $\text{Nd}_{0.75}\text{Sr}_{0.25}\text{FeO}_{2.99}$.

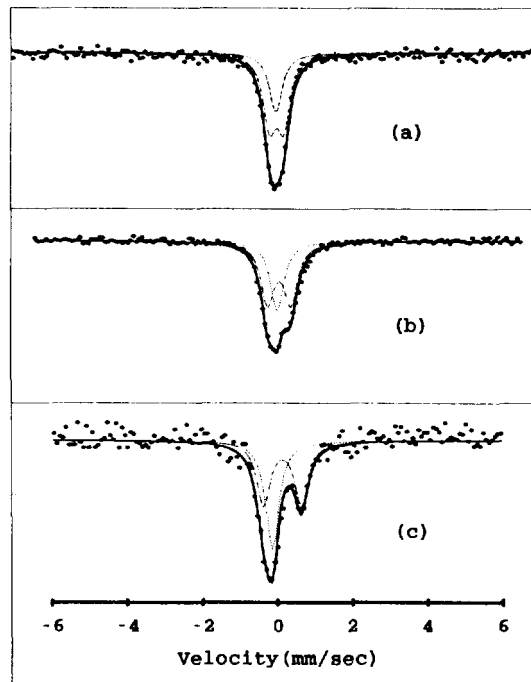


Figure 3. Mössbauer spectra for the $\text{Nd}_{1-x}\text{Sr}_x\text{FeO}_{3-y}$ system at the room temperature: (a) $\text{Nd}_{0.50}\text{Sr}_{0.50}\text{FeO}_{2.94}$, (b) $\text{Nd}_{0.25}\text{Sr}_{0.75}\text{FeO}_{2.85}$, and (c) $\text{SrFeO}_{2.73}$.

Table 3. Mössbauer Parameters for the $\text{Nd}_{1-x}\text{Sr}_x\text{FeO}_{3-y}$ System

x	Fe (type)	Isomer shift (± 0.001 mm/sec)	Quadrupole splitting (± 0.002 mm/sec)	Internal field (± 5 kOe)
0.00	Fe^{3+}	0.362	0.017	518
0.25	Fe^{3+}	0.304	0.069	514
	Fe^{4+}	-0.078	—	—
0.50	Fe^{3+}	0.159	0.194	—
	Fe^{4+}	-0.032	—	—
0.75	Fe^{3+}	0.150	0.522	—
	Fe^{4+}	-0.017	—	—
1.00	Fe^{3+}	0.166	0.938	—
	Fe^{4+}	-0.180	—	—

wmillerite to the perovskite cubic structure, which has been proposed by Takeda *et al.*¹⁴ The transition takes place due to the existence of a small amount of the brownmillerite type structure within the cubic phase.

The Mössbauer spectra recorded at room temperature for the $\text{Nd}_{1-x}\text{Sr}_x\text{FeO}_{3-y}$ system are shown in Figures 2 and 3. The Mössbauer parameters such as isomer shift (δ), quadrupole splitting (E_Q), and internal magnetic field (H_{int}) are listed in Table 3. The Mössbauer spectrum of $\text{NdFeO}_{3.00}$ represents only Fe^{3+} ion and the other compounds show complex spectra depending upon the mixed valence state between the Fe^{3+} and Fe^{4+} ions in good agreement with the result of Mohr salt analysis.

The spectrum of the composition of $x=0.00$ shows a 6-lines which is produced by only hyperfine splitting of Fe^{3+} ions in an octahedral site. The compound of $x=0.25$ contains a single line of Fe^{4+} ion as well as a 6-lines of Fe^{3+} ion. There is an antiferromagnetic interaction of $\text{Fe}^{3+}-\text{O}^{2-}-\text{Fe}^{3+}$ in the compounds of $x=0.00$ and 0.25. The Fe^{3+} ions located

in octahedral site are magnetically ordered by the indirect interaction through the bridging oxygen ions in the room temperature. The compounds of $x=0.50$, 0.75, and 1.00 exhibit double lines and a single line due to Fe^{3+} and Fe^{4+} ions, respectively. The Fe ions of the compounds are not magnetically ordered in the room temperature.

The quadrupole splitting of Fe^{3+} ion increases with x -value in the compositions of $x \geq 0.50$. The more amount of oxygen vacancies may produce the larger the electrical field gradient in Fe sublattice of the perovskite compounds with the increasing quadrupole splitting of Fe^{3+} ion. Since there are a large amounts of oxygen vacancies and Fe^{4+} ions in the composition of $x=1.00$, the quadrupole splitting of Fe^{3+} ion is larger than that of $x=0.50$. In spite of large amounts of

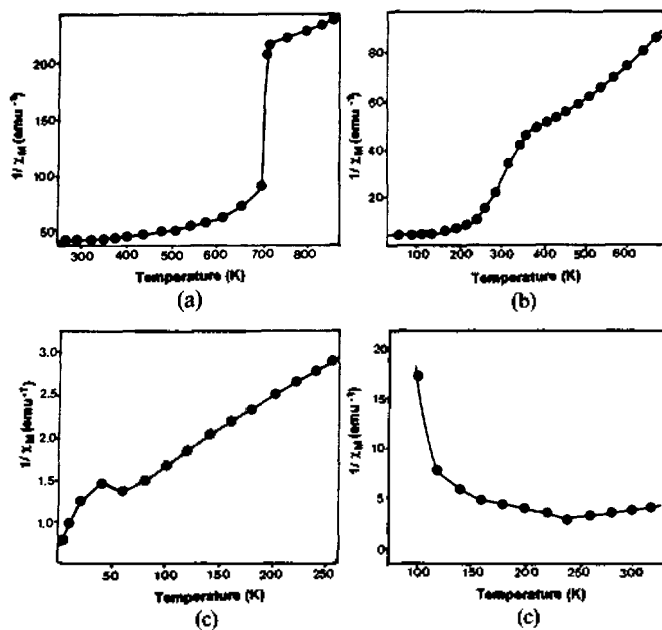


Figure 4. Plot of $1/\chi_M$ vs. temperature for the $\text{Nd}_{1-x}\text{Sr}_x\text{FeO}_{3-y}$ system: (a) $\text{NdFeO}_{3.00}$, (b) $\text{Nd}_{0.75}\text{Sr}_{0.25}\text{FeO}_{2.99}$, (c) $\text{Nd}_{0.25}\text{Sr}_{0.75}\text{FeO}_{2.85}$, and (d) $\text{SrFeO}_{2.73}$.

oxygen vacancies, there is no discrete peak induced by the Fe ions placed in the tetrahedral and the octahedral sites, respectively. It is ascribed to the oxygen vacancies that are not ordered differing from the $\text{CaFeO}_{2.50}$.¹⁵

The e_g electron of Fe^{3+} ion is transferred to the empty e_g orbital of Fe^{4+} ion by $\text{Fe}^{3+}-\text{O}^{2-}-\text{Fe}^{4+}$ bond via an intervening oxygen ion. The interaction induces high s -electron density at the nucleus of Fe^{3+} ion because of lower shielding effect of the d -electron. Thus the isomer shift of Fe^{3+} ion decreases as the amount of Fe^{4+} ion increases. The isomer shift of Fe^{3+} ion between the compositions of $x < 0.50$ and $x \geq 0.50$ shows a large difference. In the compounds of $x \geq 0.50$, the peaks of a singlet and a doublet are overlapped due to fast electron transfer between the Fe^{3+} and Fe^{4+} ions, which induce electron density to vary at the nucleus of the Fe ion. The e_g electrons of Fe^{3+} ions are delocalized over all the Fe ions, which is made possible by indirect interaction between the Fe ions in $x \geq 0.50$.

The reciprocal magnetic susceptibility as a function of temperature are shown in Figure 4. All of the samples are antiferromagnetically coupled between Fe ions below the Néel temperature. The Néel temperature of the compounds of $x = 0.00$ and 0.25 are 710 and $350(\pm 5)$ K, respectively. Their antiferromagnetic interaction exhibits a weak ferromagnetism due to the spin canting induced by a distortion of FeO_6 sublattice in the orthoferrite type structure. The compound of $x = 0.00$ containing only Fe^{3+} ion has a strong antiferromagnetic interaction of $\text{Fe}^{3+}-\text{O}^{2-}-\text{Fe}^{3+}$ and a high Néel temperature. However, the Fe^{4+} ions produced by replacing the Nd^{3+} ions with the Sr^{2+} ions interrupt the $\text{Fe}^{3+}-\text{O}^{2-}-\text{Fe}^{3+}$ antiferromagnetic interaction. Thus the magnetic transition temperature is decreased with the increasing x -value. The Néel temperature of compounds of $x = 0.75$ and 1.00 are 60 and $240(\pm 5)$ K, respectively. Thus Mössbauer spectra for the compounds of $x \geq 0.50$ do not show 6-lines splitting at room

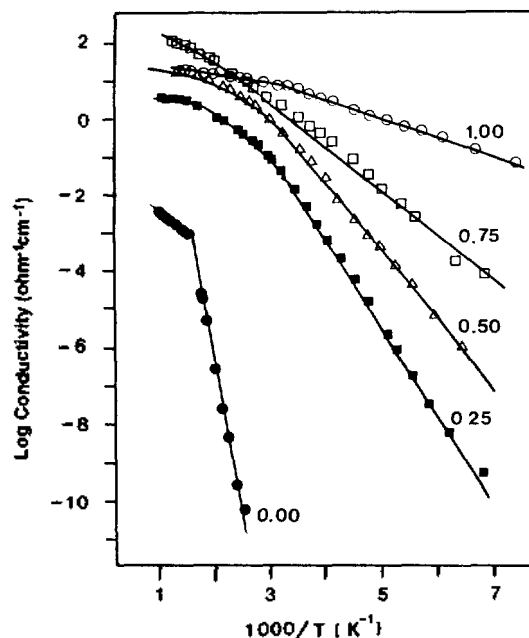


Figure 5. Plot of log electrical conductivity vs. $1000/T$ for the $\text{Nd}_{1-x}\text{Sr}_x\text{FeO}_{3-y}$ system.

Table 4. Activation Energy of the Electrical Conductivity for the $\text{Nd}_{1-x}\text{Sr}_x\text{FeO}_{3-y}$ System

x value	Temperature range (K)	Activation energy (eV)
0.00	$78 \leq T \leq 560$	1.59(3)
	$560 \leq T \leq 940$	0.23(1)
0.25	$78 \leq T \leq 320$	0.42(1)
	$320 \leq T \leq 580$	0.18(1)
0.50	$78 \leq T \leq 360$	0.31(1)
0.75	$78 \leq T \leq 490$	0.22(2)
1.00	$78 \leq T \leq 430$	0.09(1)

temperature.

The plots of the log conductivity vs. $1000/T$ are presenting a good linearity at low temperature region as shown in Figure 5. The activation energies of the conductivity obtained by the Arrhenius plots are listed in Table 4. The activation energy for the composition of $x = 0.00$, $\text{NdFeO}_{3.00}$, is very high, 1.59 eV, in the temperature below 690 K. The transition temperature of the plot is similar to the magnetic transition temperature ($T_N = 710$ K). The electrons of the Fe^{3+} ions are localized and their spins are magnetically ordered through the indirect interaction below the transition temperature. Therefore, it leads to the difficulty of the electron transfer and the high activation energy in $\text{NdFeO}_{3.00}$.

However, the activation energy decreases rapidly with the increasing x -value. The activation energy depends mainly on the concentration of the Fe^{4+} ion containing the empty e_g orbital. The relation between the activation energy and x -value is plotted in Figure 6. The e_g orbital of the Fe-ion is overlapped with p -orbital of oxygen ion. The overlap of σ -bonding character is formed in a certain range and is apt

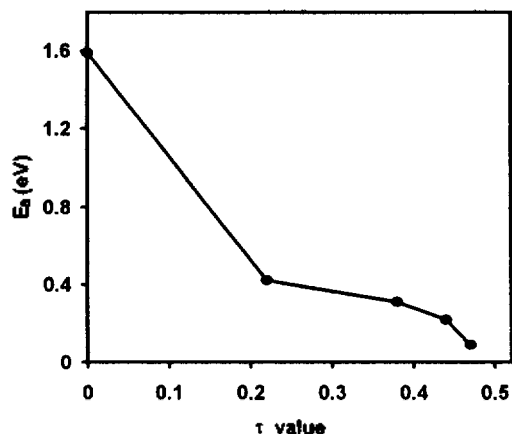


Figure 6. Plot of the activation energy vs. τ value for the $\text{Nd}_{1-x}\text{Sr}_x\text{FeO}_{3-y}$ system.

to electron transfer. The electron transfer from e_g electron of the Fe^{3+} ion to the empty e_g orbital of the Fe^{4+} ion results in the higher electrical conductivity and the lower activation energy.

Finally, the indirect interaction between Fe ions is made possible through σ bonding character of $e_g(\text{Fe})-p(\text{O})-e_g(\text{Fe})$ in the perovskite compounds. From the Mössbauer spectroscopy and the electrical conductivity measurement, it is found out that the electron transfer is very fast by the indirect interaction between Fe ions in the case of the sample containing a large amount of Fe^{4+} ion. Since the e_g electrons are delocalized over all the Fe ions for the compositions of $x \geq 0.50$ containing a large amount of Fe^{4+} ions, it leads to the overlap of the peaks of the Fe^{3+} and Fe^{4+} ions in the Mössbauer spectra and the decrease of the activation energy for the electrical conductivity.

Acknowledgments. This work was supported by Granted No. 92-25-00-02 from the Korea Science and Engi-

neering Foundation in 1992 and therefore we express our deep appreciation to the authorities concerned.

References

1. Taguchi, H.; Shimada, M.; Koizumi, M. *J. Solid State Chem.* **1982**, *41*, 329.
2. Yo, C. H.; Lee, E. S.; Pyun, M. S. *J. Solid State Chem.* **1988**, *73*, 411.
3. Ryu, K. H.; Roh, K. S.; Lee, S. J.; Yo, C. H. *J. Solid State Chem.* **1993**, *105*, 550.
4. Buffet, B.; Demazeau, G.; Pouchard, M.; Dance, J. M.; Hagemuller, P. *J. Solid State Chem.* **1983**, *50*, 33.
5. Joo, G. T.; Ravez, J.; Grenier, J. C.; Hagemuller, P. *Mat. Res. Bull.* **1986**, *21*, 535.
6. Yo, C. H.; Jung, S. T.; Pyun, W. B.; Lee, S. H. *J. Kor. Chem. Soc.* **1989**, *33*(5), 445.
7. Trevs, D. *Phys. Rev.* **1967**, *156*, 562.
8. Takano, M.; Kawachi, J.; Nakanishi, N.; Takeda, Y. *J. Solid State Chem.* **1981**, *39*, 75.
9. Takeda, T.; Yamaguchi, Y.; Watanabe, H. *J. Phys. Soc. Japan* **1972**, *33*, 967.
10. Oda, H.; Yamaguchi, Y.; Takei, H.; Watanabe, H. *J. Phys. Soc. Japan* **1977**, *42*, 101.
11. Gibb, T. C. *J. Chem. Soc. Dalton Trans.* **1985**, 1455.
12. Hombo, J.; Matsumoto, Y.; Kawano, T. *J. Solid State Chem.* **1990**, *84*, 138.
13. Takano, M.; Okita, T.; Nakayama, N.; Bando, Y.; Takeda, Y.; Yamamoto, O.; Goodenough, J. B. *J. Solid State Chem.* **1988**, *73*, 140.
14. Takeda, Y.; Takeno, K.; Takada, T.; Yamamoto, O.; Takano, M.; Nakayama, N.; Bando, Y. *J. Solid State Chem.* **1986**, *63*, 237.
15. Grenier, J. C.; Pouchard, M.; Hagemuller, P. *Structure and Bonding* **47**; Springer-Verlag: Berlin, Heidelberg, New York, 1981; p 2.